MODELING INTERGRANULAR FRACTURE AT ELEVATED TEMPERATURE

By

Muhammad Akmalhazwan Bin Ahmad Kamil

Dissertation submitted in partial fulfillment of

the requirements for the

Bachelor of Engineering (Hons)

(Mechanical Engineering)

SEPTEMBER 2012

Universiti Teknologi PETRONAS

Bandar Seri Iskandar

31750 Tronoh

Perak Darul Ridzwan

CERTIFICATION OF APPROVAL

MODELING INTERGRANULAR FRACTURE AT ELEVATED TEMPERATURE

by

Muhammad Akmalhazwan Bin Ahmad Kamil

A project dissertation submitted to the

Mechanical Engineering Program

Universiti Teknologi PETRONAS

in partial fulfillment of the requirement for the

Bachelor of Engineering (Hons)

(Mechanical Engineering)

Approved by,

_____

(Dr Azmi Bin Abdul Wahab)

Date:

UNIVERSITI TEKNOLOGI PETRONAS

TRONOH, PERAK

SEPTEMBER 2012

CERTIFICATION OF ORIGINALITY

This is to certify that I, Muhammad Akmalhazwan Bin Ahmad Kamil (I/C No: 890605-05-5483), am responsible for the work submitted in this project, that the original work is my own except as specified in the references and acknowledgements, and that the original work contained herein have not been undertaken or done by unspecified sources or persons.

_____

MUHAMMAD AKMALHAZWAN BIN AHMAD KAMIL

Student ID : 13497

I/C No : 890605-05-5483

Date :

ABSTRACT

This project aimed to produce numerical models for intergranular fracture at elevated temperature as continuation of the work by Rishi Raj and M.F. Ashby [1]. They have been studying about intergranular fracture caused by void formation mainly on homogenous copper. As one of the most referred journal in intergranular fracture at elevated temperature, working numerical models on other materials have not yet been made available. Upon completion of the numerical model, it will be then applied to other materials and applications that are exposed to intergranular fracture at elevated temperature. This project is divided in two main sections; to build a numerical model for nucleation of voids and the growth of voids. Even though there are many types of creep failures, the project will be centered only on creep failure as a result of nucleation, growth and coalescence of voids. The work will reproduce the model of nucleation and growth based on copper data as in the work of Raj and Ashby [1] and then to apply the models to other materials. It is anticipated that with the nucleation and growth models, estimation of rupture time of a material at elevated temperature can be reliably predicted. It is important not to confuse between intergranular fracture caused by void nucleation, growth and coalescence and intergranular fracture caused by boundary cracking. Major difference between these two is intergranular fracture caused by void formation occur in low stress, elevated temperature environment whereas intergranular fracture caused by boundary cracking is due to high stress exerted to the material.

ACKNOWLEDGEMENT

Thanks to God, who with His willing, gives me the chance to complete this Final Year Project. First and foremost, I would like to express my deep appreciation to my supportive supervisor Dr Azmi Bin Abdul Wahab, who has guided and support me during these two semester sessions to complete this project.

I would also want to thank all lecturers and staffs of Mechanical Engineering for their co-operations, suggestions and time responding to my inquiries along the way. Dearest thanks and appreciation to my beloved parents, Ahmad Kamil Harun and Misliah Masari, for their love, support and prayers throughout my time completing this project.

Not to forget, to all my friends and for their cooperation, encouragement, constructive suggestion and full of support for this project completion, from the beginning till the end. My gratitude to everyone who has been contributing by supporting my work for the period of the final year project progress till it is completely completed.

TABLE OF CONTENT

LIST OF TABLES

LIST OF FIGURES

CHAPTER 1

1. INTRODUCTION

1.1 Background of Study

Materials exposed to stresses at high working temperature normally will slowly deform permanently in a condition that is called creep. Creep occurs due to various reasons and this project will be focusing on creep failures caused by the nucleation, growth and coalescence of voids in the grain boundaries. One such creep failure occurs in steam methane reformers where growth and coalescence of voids leads to rupture of the tubes.

This study adapted Rishi Raj and M. F. Ashby's work of homogenous copper material to build a numerical model based on it. Their study are consisted the analysis of intergranular fracture based on unifying void configurations with various parameters such as grain size, temperature, strain rate, diverse interface energies and size and density of second phase particles in the boundary [1].

1.2 Problem Statement

Various researchers have provided analytical equations to study the failure of materials at elevated temperature. Therefore, computer model is crucial to forecast and investigate the failure of materials when they are exposed to high temperature environment. Since Rishi Raj and M.F. Ashby work is among the most cited, adaption of the study and numerical models should be made available for use on other material systems. With this program and appropriate material properties, the behavior of materials at elevated temperature can be predicted.

1.3 Objectives

The main objective of this project is to adapt a numerical model based on work by Rishi Raj and M. F. Ashby [1]. The computer model will employ analytical equation given in the work by Raj and Ashby.

Based on the numerical model produced, it will be used to replicate the result obtained by Rishi Raj and M. F. Ashby [1] on homogenous copper material and generate the void nucleation and growth curves.

After replicating the result obtained by Rishi Raj and M. F. Ashby [1], the numerical model will then be used to analyze the nucleation, growth and coalescence of void in industrial application, specifically in steam methane reformer.

1.4 Scope of Study

The output of the model is time to rupture for material subjected to stress at high temperature. The model deals one type of creep failure, which is nucleation, growth, and coalescence of voids at elevated temperature. This work will be performed in materials where suitable material constants are used and tested.

1.5 The Relevancy of the Project

This project could also provide critical analysis towards the nucleation, growth and coalescence of voids model in which its concept, limitation and exception can be better understood. The analysis process that is supported with experimental data will be able to improve author's ability to make significant reasoning.

CHAPTER 2

2. LITERATURE REVIEW

2.1 Creep Failure

Creep is defined as the time-dependent deformation and it caused permanent deformation when load or stress is applied continuously to materials. Creep is typically material deformation that occurred when the material is exposed to static mechanical stress at elevated temperature, such as the sagging phenomenon of tungsten light bulb filaments. When the filament is induced with electrical flow, the filament gets heated and the sagging cause by its own weight between its supports increased. When the deformation caused by stresses of its weight and high temperature is too much, the deformations will immediately lead to failure of the filaments. Creep in general is an unwanted event and it is usually the restraining factor in the longevity life span of a part. When materials are at temperatures larger than $0.4T_m$ where T_m is the absolute melting point of the material, creep is observed [2].

Creep is an important consideration in design in three types of high temperature applications, which are [3]:

- the displacement-limited applications in which precise dimensions or small clearances must be maintained such as in turbine rotors in jet engines;
- rupture-limited applications in which precise dimensions are not essential but fracture must be avoided such as in high pressure steam tubes and pipes;
- stress-relaxation-limited applications in which an initial tension relaxes with time such as in suspended cables and tightened bolts.

Engineers must take into consideration creep deformation and its dependence on time and temperature when designing system concerning with the three type of creep applications. Numbers of mechanical systems and components like steam boilers, turbines, and reactors operate at high temperatures and hence, it is essential for creep properties of respective materials used to be analyzed.

Creep stages can be divided into three, which are primary creep, steady state creep and tertiary creep. These stages can be explained more by using the graph below [4].

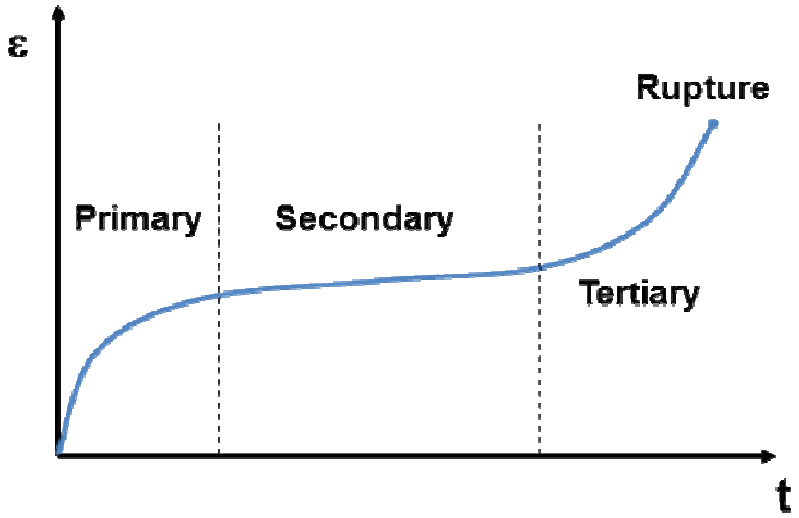

Figure 2.1: Creep curve of strain [4].

Based on the graph above:

1. Primary creep: Where the rate of change of strain (creep rate=$\Delta\varepsilon/\Delta t$) decreases with time due to strain hardening of the material.

2. Secondary creep: Where the strain increases linearly with time. From design point of view, this region is the most important one for parts designed for long service life because it comprises the longest creep duration. The main creep test result is the slope of this region, which is known as the steady-state creep rate. During this stage of creep, there is a balance between strain hardening due to deformation and softening due to recovery processes similar to those

occurring during the annealing of metals at elevated temperature.

3. Tertiary-creep: Where the strain increases rapidly until failure or rupture. The time to failure is often called the time to rupture or rupture lifetime (t_r). This parameter is an important consideration in designing against creep for parts intended for short-life applications. To determine the rupture lifetime, the creep test must be conducted to the point of failure.

2.2 Steam Methane Reformer

The steam reformer is a vital part of hydrogen plants and of the gas preparation section in plants producing ammonia, methanol, and other types of synthesis gas. The advancement in metallurgy has enable steam reformer to be made of materials that can withstand higher temperature. For instance, in steam methane reforming process, at high temperature of about 700˚C to 1000˚C, steam reacts with methane to produce carbon monoxide and hydrogen [5].

Figure 2.2 [10] below shows steam methane reformer tubes in operation. The photo was taken with thermography technique:

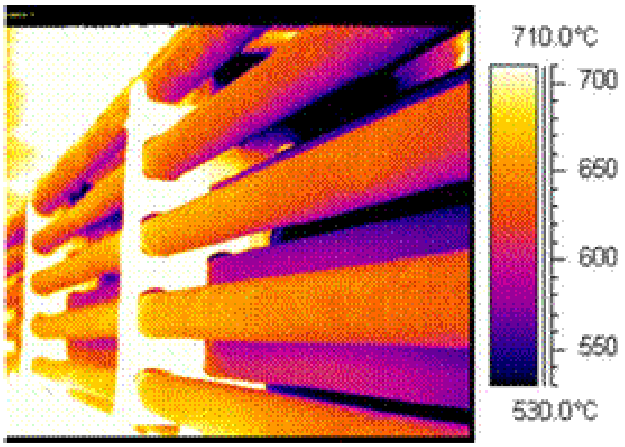

Figure 2.2: SMR Tubes in Operation [10]

In order for the reformer to function at its optimum capacity, it must be exposed to elevated working temperature. The designer can foresee the expected service life by means of suggesting the working temperature of the reformer by

referring to creep rupture curves. However, a little raise or reduction in the tube metal temperature will severely reduce service life and the cost [6]. For example, 40 degrees Celsius higher will add unnecessary thickness by 40% and 40 degree Celsius lower will significantly reduce its expected life from 10 years to actual life of 1 ½ years [6].

Figure 2.3 [10] below shows a SMR that has been undergone creep effect known as sagging due to its own weight in elevated temperature environment:

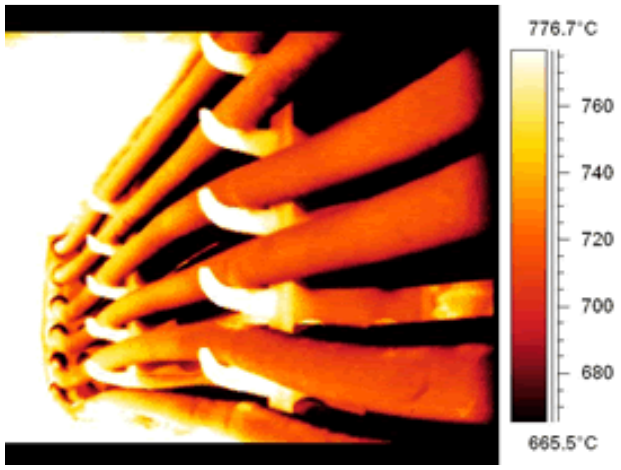

Figure 2.3: Sagging Phenomenon of SMR tubes at High Temperature [10]

For this reason, the model of intergranular fracture at elevated temperature is needed so designers and engineers can reliably predict and calculate the time to rupture of materials so the application can be lengthen and the process can be optimized.

2.3 Creep Due to Void Nucleation and Growth

Nucleation, growth and coalescence of voids are the major factor in ductile failure mechanism. Basically it is an outcome of de-bonding or cracking at the particles level of a material. Initially, elevated temperature will kick off the nucleation of the void. The voids then start to develop after a period of time. Each void will grow bigger and bigger along granular boundaries which then meet and combine and finally results in rupture of materials.

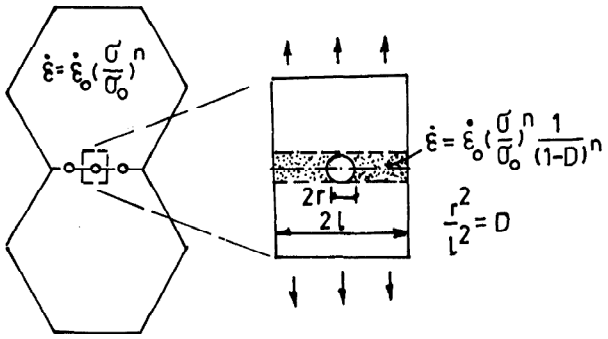

Figure 2.4: Schematic diagram of growth.[1]

Based on the schematic diagram figure 2.4 above, both trans-granular and intergranular voids growth in power law creep is possible and the place of the event occur will affects the void's dimension. The voids grow and stabilized with time dependent manner. By the time when the voids achieved their ultimate size, the stress on the remaining area of cross-section will reach the maximum stress at the temperature and rupture will occur [7].

In this study, the two functions that will be used to develop growth and nucleation models are as below [1]:

The time to rupture for fixed number of nuclei, t_r:

$$t_r = \frac{3\sqrt{\pi}}{32} \frac{kT}{\Omega D_B \delta} \frac{1}{(\sigma_\infty - p)\rho^{3/2}} \frac{F_V(\alpha)}{{F_B}^{3/2}} \int_{A_{min}}^{A_{max}} \frac{dA}{f(A)}$$

According to the equation above,

- t_r is the time to rupture for fixed number of nuclei.
- $\frac{kT}{\Omega D_B \delta}$ is the diffusity rate for the time to rupture.
- k is Boltzman constant.
- T is temperature.
- Ω is the atomic volume of the material.
- D_B is the grain boundary self diffusion coefficient.
- δ is the boundary thickness.
- σ_∞ is the external applied load exerted on the void per unit area.

- p is the internal pressure.
- F_V is the function of angles that provide void's volume.
- ${F_B}^{3/2}$ is the function of energy that provide the area B.
- $\int_{A_{min}}^{A_{max}} \frac{dA}{f(A)}$ is limitation to the possible nucleation sites.

A_{max} is the upper limit set to the value of 0.5 since that is the maximum value possible for void density occupying the grain boundary area. Any value larger than that will lead to the failure of the material.

The time to rupture for continuous void nucleation:

$$0.5 = \frac{3\sqrt{\pi}}{32}\frac{\Omega D_B \delta}{kT}\sigma_\infty \frac{F_B^{\frac{3}{2}}(\alpha)}{F_V(\alpha)}\int_0^{tr}\int_\tau^{tr} \rho^{\frac{1}{2}}(t-\tau)\dot{\rho}(\tau) f\big(A(t-\tau)\big)dtd\tau$$

According to the equation above,

- 0.5 is the limitation value of which maximum void density allowable for before the material fail.
- ρ is void density of the number of void per unit area in the grain boundary.
- $\dot{\rho}$ is the nucleation rate.

Value of 0.5 is the limitation for the void density, as the material will fail whenever the calculated value is bigger or equal to itself.

2.4 Void Geometries

There are various types of void geometries as they can form at two-grain, three-grain and four-grain junctions. The common features are the free surfaces of the void are spherical segments and the angle between the void must satisfy equilibrium between the surface tension [8].

There are two categories of voids. The first category is voids in inclusion-free boundaries and the second is voids at inclusions. The inclusion-free boundaries normally lead to sliding grain boundaries. Apart from that, as shown on figure 2.5

and figure 2.6, voids exist as Type A and Type B voids. The differences are that for Type A, the void lies entirely on the inclusion-matrix interface, whereas for Type B, the voids broaden into the grain boundaries [1]. Both types are shown in the two figures below.

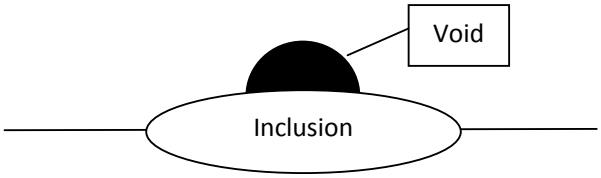

Figure 2.5: Type A of void that can form at inclusion. [1]

Figure 2.6: Type B of void that can form at inclusion. [1]

In order to identify the time to fracture of the material, growth of the void is estimated beforehand. Figure 2.7 shows that voids are assumed to be certain number and regularly positioned in an array manner.

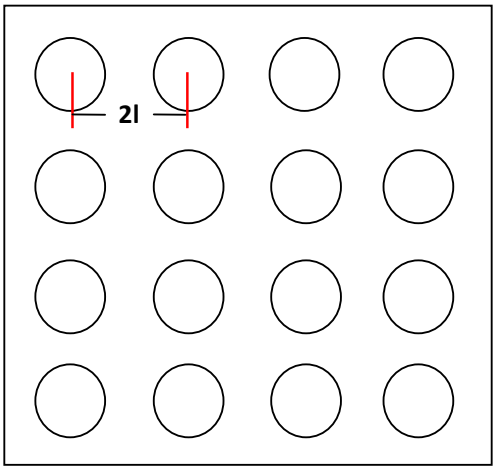

Figure 2.7: Periodic array of voids in grain boundary. [1]

In actual fact, the assumptions are made to ease calculation later as there is no way to definitely get the correct value. Stress or load at elevated temperature applied to the material will cause nucleation of voids, followed by voids growth and the material will fail because of tearing between the growing voids and deformation occurred.

CHAPTER 3

3. METHODOLOGY

3.1 Work Flow

In order to achieve the outlined objectives, the project is carried on by reviewing Rishi Raj and M.F. Ashby's work to achieve crucial information regarding the task. Information from other sources such as journals, textbooks and articles are collected as much as possible. This is one of the important phases where clearer picture on equations used can be obtained.

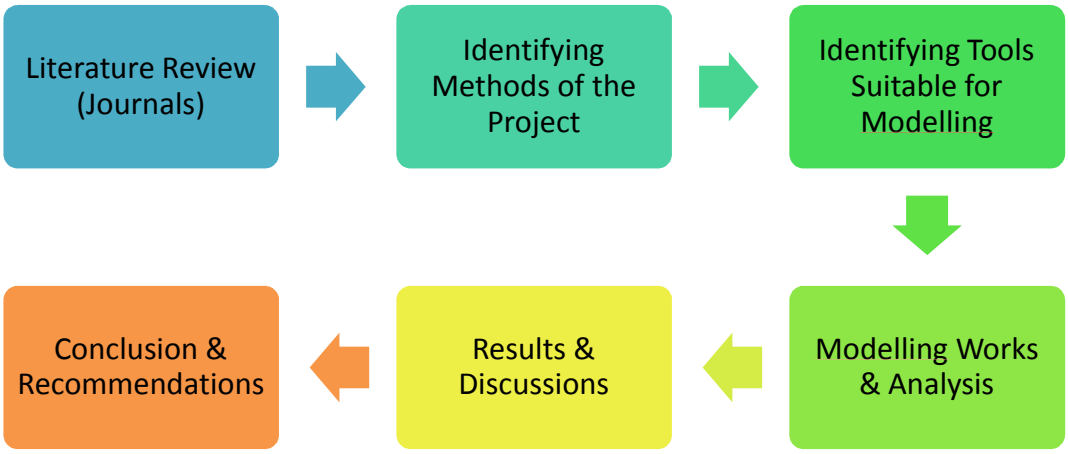

Figure 3.1: Final Year Project's Work Flow

With the sufficient data collected, methods of the project are determined. These include determining the modeling software and step-by-step progression of the project. For this project, two software are being used namely Microsoft Excel together with addition of Visual Basic for Application. Both software were used to calculate and analyze the data.

3.2 Flow Chart

The project serves as continuation of the Rishi Raj and M.F. Ashby to gain information regarding intergranular fracture at elevated temperatures. In order to understand the equations and models better, and to be able to work smoothly, information from journals and books are collected as much as possible as reference in completing the work.

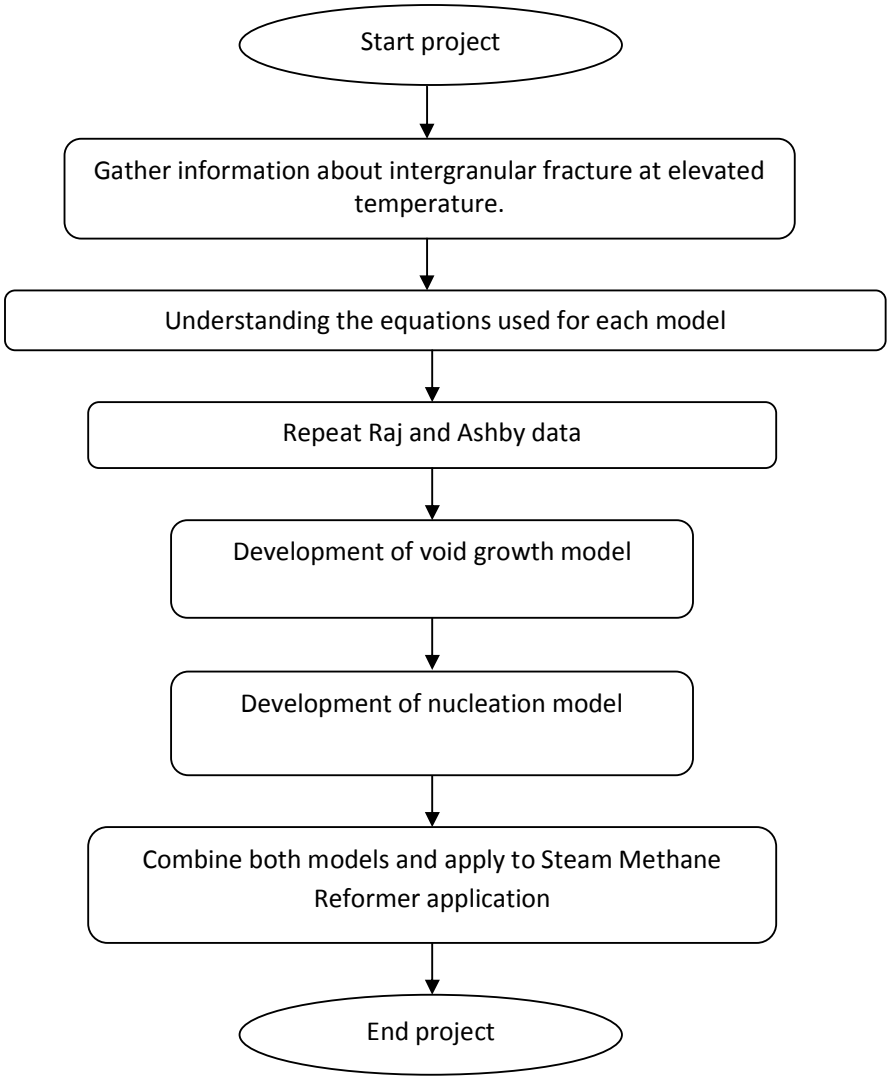

Figure 3.2: Flow chart for the project.

Subsequently, Microsoft Office Excel is used to calculate all of the equation and data gathered. The work will be started with modeling time to fracture with fixed number of nuclei. Then the work will proceed with the modeling of time to fracture with continuous nucleation and no grain boundary sliding.

Modeling progress will be done using data that has been used by Rishi Raj and M.F Ashby. The aim is to replicate the result of their study so that it is confirmed that numerical models that has been developed were correct.

After succeed in replicating Rishi and Ashby data, the models will be tested for Steam Methane Reformer application. By the time models for the study completed, they will then be tested with data for other materials to ensure that both models have been developed accordingly.

3.3 Tool

Microsoft Office Excel will be used as the main tool to develop the program for modeling of intergranular fracture at elevated temperature. The software is chosen because of its user-friendly interface. In addition, changes to the input data can be easily incorporated and any graphs produced by the software are easily updated. Furthermore, the software provides a number of predefined functions and allows user to develop new function to cope with the user's need.

3.4 Gantt Chart

Table 3.1: Gantt Chart for FYP

ACTIVITIES	SEMESTER I														SEMESTER II												
	1	2	3	4	5	6	7	8	9	10	11	12	13	14	1	2	3	4	5	6	7	8	9	10	11	12	13	14
Background of Study																												
Literature Review																												
Development of Void Growth Model																												
Improvement of Void GrowthModel																												
Development of Nucleation Model																												
Improvement of Nucleation Model																												
Improvement of Models																												
Extended Proposal Submission																												
Proposal Defence																												
Interim Report Submission																												
Progress Report Submission																												
Poster Presentation																												
VIVA																												
Technical Paper																												
Dissertation																												
Documentation																												

Progress of the whole FYP work is shown by the Gantt chart table above. The important dates and the key milestones are noted by the star symbol. The significant of the symbols are the mark of all the documentations submission dates and the major final year project's progress of Modeling Intergranular Fracture at Elavated Temperature.

3.5 Modeling Time to Rupture: Fixed Number of Nuclei

The work is divided into two parts, one is nucleation and another is growth. Both require development of codes to ensure that the integration part in the formulation can be calculated. Both developments of codes are shown in details below.

3.5.1 Model Development Steps

The parameters for equation of time to rupture for fixed number of nuclei can be obtained from the data table. The complicated part is at the integration section where lines of codes need to be written in order to accomplish the calculation on the part. The codes for the part are shown in section 3.5.2 below.

3.5.2 Codings

```
'Coding of Void Growth Model
' Integration function : dA/f(A)
        Function inverse_fA(a, rc, r) – to inverse the function of fA/ 1/fA
Const e = 2.718281828 – Constant
inverse_fA = a ^ 0.5 * (0.5 * Log(1 / a) / Log(e) - 0.75 + a * (1 - a / 4)) / ((1
        - rc / r) *
        (1 - a))
 End Function
' Iteration for single intergration
        Function integrate_inverse_fA(Amax, Amin, n, l, Fb, rc)
Const pi = 3.141592654
        h = (Amax - Amin) / n
sum_odds = 0 - set the initiation value
sum_evens = 0 - set the initiation value
A_odds = A_min + h
'Coding for iteration loop for single integration
        For i = 1 To n - 1 Step 2
        r = (pi * A_odds * l ^ 2 / Fb) ^ 0.5
sum_odds = sum_odds + inverse_fA(A_odds, rc, r)
A_odds = A_odds + 2 * h
        Next i
A_evens = A_min + 2 * h
        For j = 2 To n - 2 Step 2
        r = (pi * A_evens * l ^ 2 / Fb) ^ 0.5
        sum_evens = sum_evens + inverse_fA(A_evens, rc, r)
A_evens = A_evens + 2 * h
        Next j
        integrate_inverse_fA = h / 3 * (inverse_fA(Amin, rc, r) + 4 * sum_odds + 2
        *sum_evens + inverse_fA(Amax, rc, r))
End Function
```

3.6 Modeling Time to Rupture: Continuous Nucleation, No Grain Boundary Sliding

3.6.1 Model Development Steps

Parameters for time to rupture for continuous nucleation with no grain boundary sliding can be obtained from the data table. Only for the double integration section, numerical procedure is applied through lines of codes in the Visual Basic for Application in Microsoft Excel. Lines of codes for the integration parts are shown in 3.6.2 below.

3.6.2 Coding

```
Function double_integration()
Const Pi = 3.412
Const e = 2.71828
Const gamma = 0.78
Const omega = 1.1E-29
Constsigma_n = 4200000
Const k = 1.38E-23
Const T = 978
Constrho_max = 1
Const rho = 1
Const FV = 0.654498469
delta_rho_i As Double
rho_dot As Double
delta_rho_dot As Double
delta_t_i As Double
A_j As Double, j As Double, i As Double
rho_dot = ((4 * Pi * gamma) / (omega ^ (4 / 3) * sigma_n)) * (1 + ((sigma_n * omega) / (k * T))) * (rho_max - rho) * (e *
(-((4 *
    gamma ^ 3 * FV) / (sigma_n ^ 2 * k * T))))
delta_t_i = 500
delta_rho_i = rho_dot * delta_t_i
    If rho_dot = 0 Then i = m End If
    Dim r(i, j) As Variant
    Dim a(j) As Variant
    Dim i As Integer
    Dim j As Integer
          a(j) = delta_rho_i * (r(i, j)) ^ 2 * Fb(a)
              For j = 1 To 50
                  For i = 1 To m
                  a(j) = delta_rho_i * (r(i, j)) ^ 2 * Fb(a)
                  If a(j) > 0.5 Then Exit For
        Else
                  If a(j) > 0.5 And j < 25 Then delta_t = delta_t + 1
        Else
                  If j >= 25 Then t_r = delta_t_k
        Else
                  If j = 50 And a(j) = 0.5 Then delta_t = delta_t + 1
        End If
   Next
Next
End Function
```

CHAPTER 4

4. RESULTS AND DISCUSSION

4.1 Data Gathering & Analysis

This work is carried out by using Raj and Ashby [1] article as the main reference to develop the numerical model in order to calculate the time to rupture of a material at elevated temperature. The article is thoroughly studied and supported with several other handbooks for data acquisition as comparison for integrity of the result obtained.

All the works is done carefully by using detailed understanding on the topic and tedious iteration of lines of codes and command in order to achieve the accurate results. The models are developed using Microsoft Office Excel with the aid of Visual Basic for Application to generate lines of codes and custom formulations.

The true aim of this project is to obtain the same graph produced in Rishi Raj and M.F Ashby article for both time to rupture of fixed number of nuclei and time to rupture for continuous nucleation and no grain boundary sliding.

4.2 Results

4.2.1 Time to Rupture for Fixed Number of Nuclei

By referring to Raj and Ashby's work, the intended models for intergranular fracture at elevated temperature are straight lines that indicate the time to rupture for the model. All the calculation and codes for fixed number of nuclei is expected to bear the result as shown in the figure below.

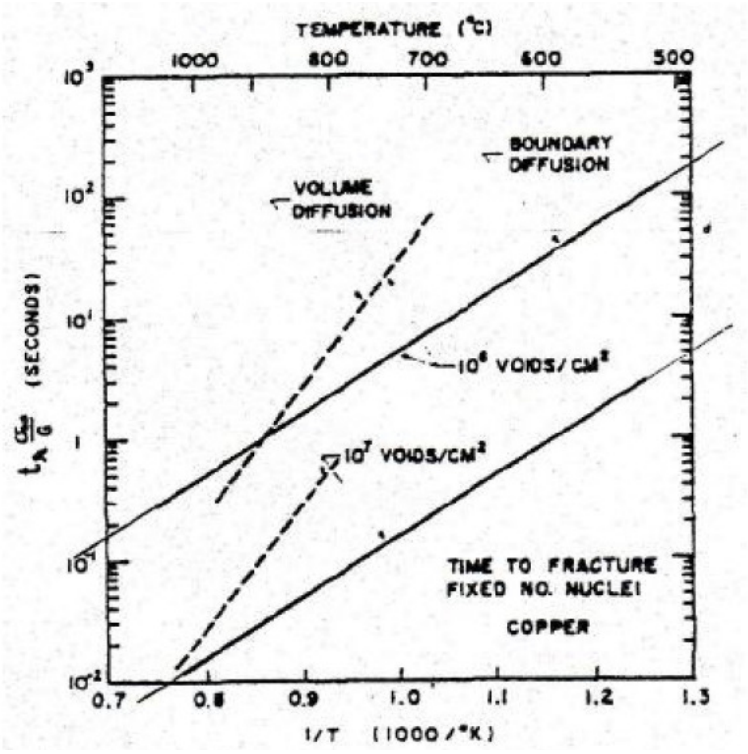

Figure 4.1: Expected Result for Fixed Number of Nuclei [1]

Based on the calculation and program that has been developed, calculations were performed from the data in appendix A.1 and the time-to-rupture for void density of 10^6 voids/cm^2 is shown in table 4.1:

Table 4.1: Modeling Data for Copper

Temperature		Time to Rupture, $T(\sigma_\infty/G)$
1/K	K	s
0.70	1429.00	0.12
0.80	1250.00	0.37
0.90	1111.11	1.16
1.00	1000.00	3.65
1.10	909.09	11.59
1.20	833.33	37.10
1.30	769.23	119.65

Based on the data obtained, graph for time to rupture is plotted. Figure 4.1 below show the results of void growth simulation. The result shown below is exactly

the same with that obtained by Ashby and Raj [1], with two different value of voids density per square centimeter. The results for 10^6 voids/cm^2 void density intersect with the Y-axis at a time to rupture value of approximately 0.1s, which is similar to the value obtained by Raj & Ashby [1].Based on this, it is assumed that the model was correctly coded.

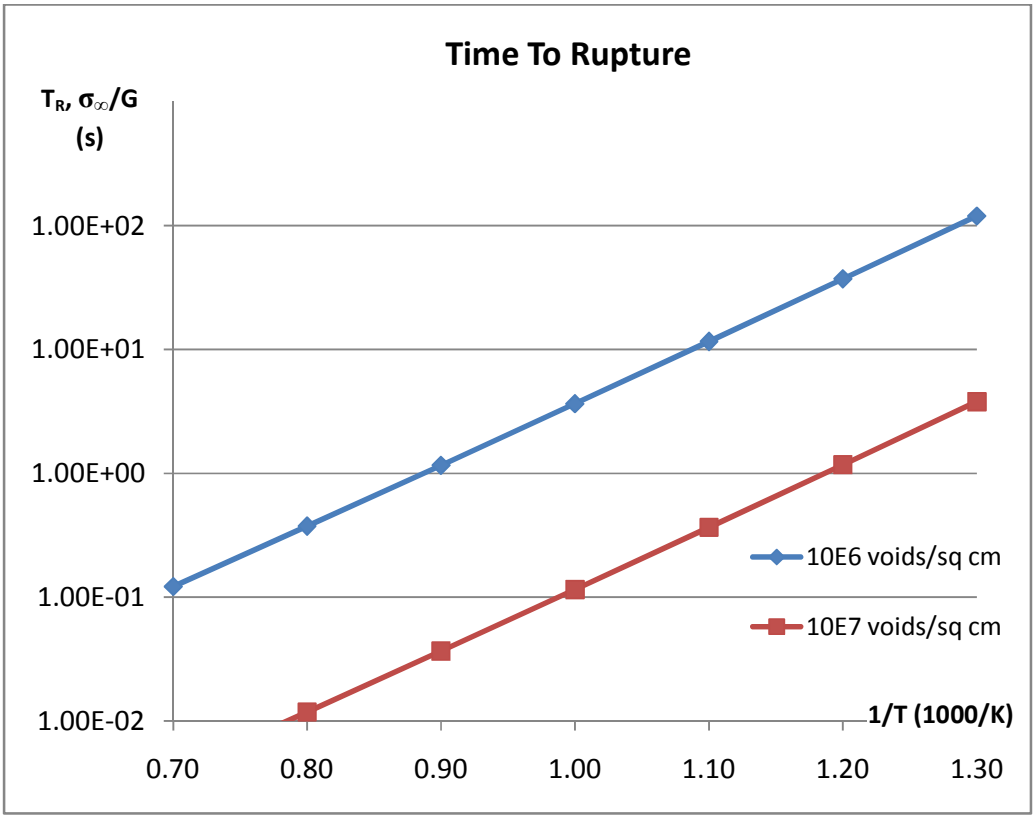

Figure 4.2: Time to rupture, fixed number of nuclei (Copper).

Figure 4.2 is the replicated model using the equation of time to rupture for fixed number of nuclei. By referring to Table 4.2, it shows the increment temperature value from 0.7 to 1.3 is actually the decrement of temperature that means the left side of the graph having higher temperature than on the right side. The values shown indicate the time taken for copper to rupture will be longer.

Other than replicating Raj & Ashby's data, data from another material were used to confirm the integrity of the result obtained.

Table 4.2: Modeling Data for Austenitic Steel

Temperature		Time to Rupture, $T(\sigma_\infty/G)$		
1/T	K	s		
		N1-I	N1-min	N1-O
0.70	1429.00	5.82	316.68	7.96
0.80	1250.00	39.24	2136.82	53.70
0.90	1111.11	267.89	14588.96	366.62
1.00	1000.00	1851.88	100850.03	2534.37
1.10	909.09	12930.91	704194.26	17696.44
1.20	833.33	91043.67	4958074.48	124596.67
1.30	769.23	645500.79	35152811.50	883391.98

Figure 4.3 show the graph obtained by using different data for austenitic steel listed in table 4.2.The calculations were based on service parameters and material constants listed in Table A2 in the Appendix. Austenitic steel is the material used in producing steam methane reformer tubes. The data represents the various locations of the steam reformer tubes. For that reason, the stress and the temperature afflicted each location are different respectively.

- N1-I is the data from inner wall of a steam reformer tubes, 2.5m from the top flange. This location is subjected to a pressure induced stress of 114MPa and temperature of 1048K.
- N1-min is the data middle section of the tube thickness, 2.5m from the top flange. This location is subjected to a pressure induced stress of 2.09MPa and temperature of 1087K.
- N1-O is the data from outer wall of a steam reformer tubes, 2.5m from the top flange. This location is subjected to a pressure induced stress of 83.1MPa and temperature of 1121K.

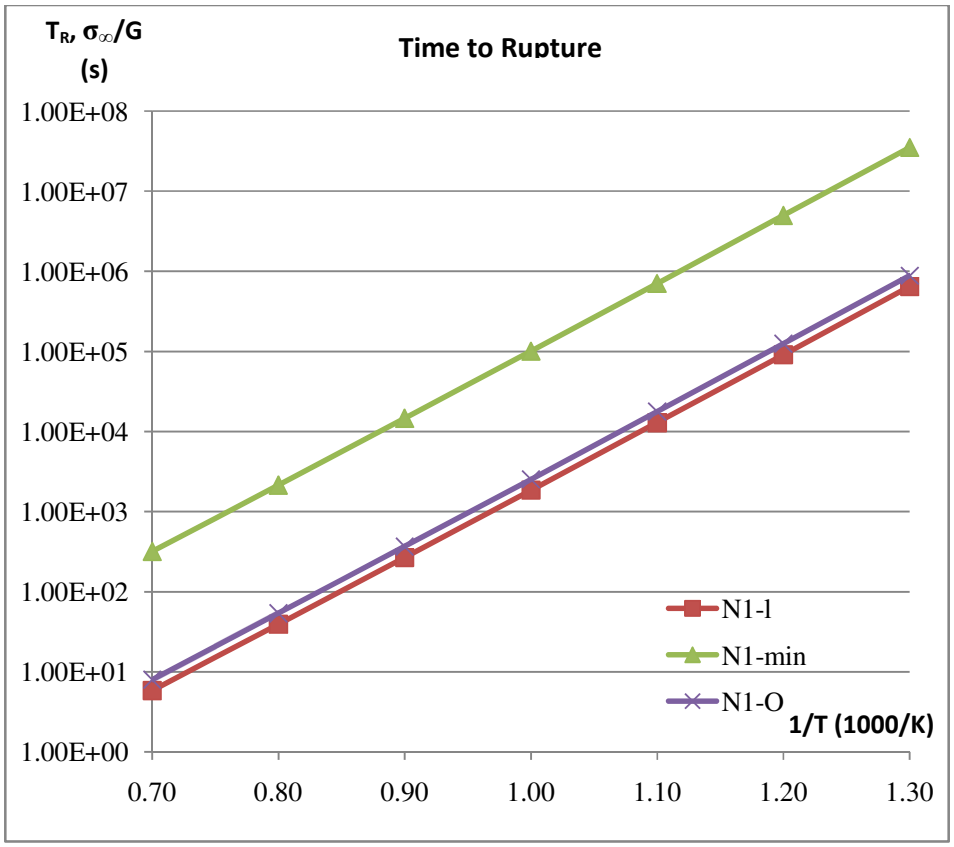

Figure 4.3: Time to rupture, fixed number of nuclei (Steel).

Three different lines in the graph indicate different locations in the steam reformer tubes. The line of time-to-rupture, in general, showed N1-min has the longest life. Upon closer inspection, the combined effect of stress and temperature resulted in N1-min location having the longest time to rupture values, whereas the higher stress value at location N1-I at the inner wall resulted in the shortest time-to-rupture value, despite the fact that the service temperature at this location is lowest. The combine effects of temperature and stress played a major role in the final time-to-rupture value, as indicated by the void growth model. Since the time-to-rupture is shortest in the internal part of the tube, failures are most likely start from inside and propagate to the outer part of the tube.

Comparing the results between the austenitic steel and copper, the austenitic stainless steel has a higher value of time to rupture. The austenitic steel has high temperature stability, enhanced creep strength, higher durability and better oxidation resistance, due to the presence of chromium alloying which also produced extensive

carbide networks,. These properties make the time to rupture for the material longer compared to copper.

4.2.2 Time to Rupture For Continuous Nucleation, No Grain Boundary Sliding.

By referring to Raj and Ashby's work, the intended model for intergranular fracture at elevated temperature is curved lines that indicate the time to rupture for the model. The expected result of the model is to bear the result as shown in the figure below.

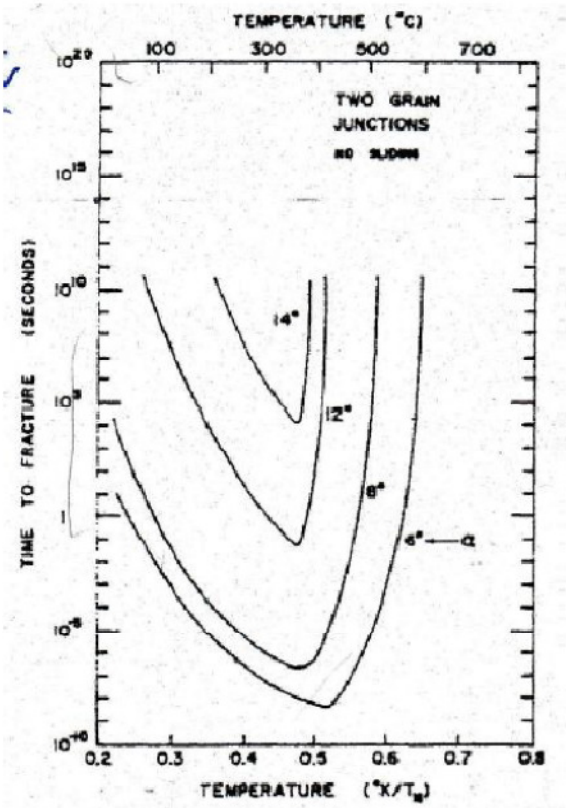

Figure 4.4: Expected result for time to rupture, continuous nucleation, no grain boundary sliding.

The results from the calculations were shown in the table below.

Table 4.3: Modeling Data for Copper

Temperature		Time to Rupture
1/T	K	s
		Copper
0.70	1429.00	6.19E+16
0.80	1250.00	2.02E+16
0.90	1111.11	6.50E+15
1.00	1000.00	2.07E+15
1.10	909.09	6.51E+14
1.20	833.33	2.02E+14
1.30	769.23	6.28E+13

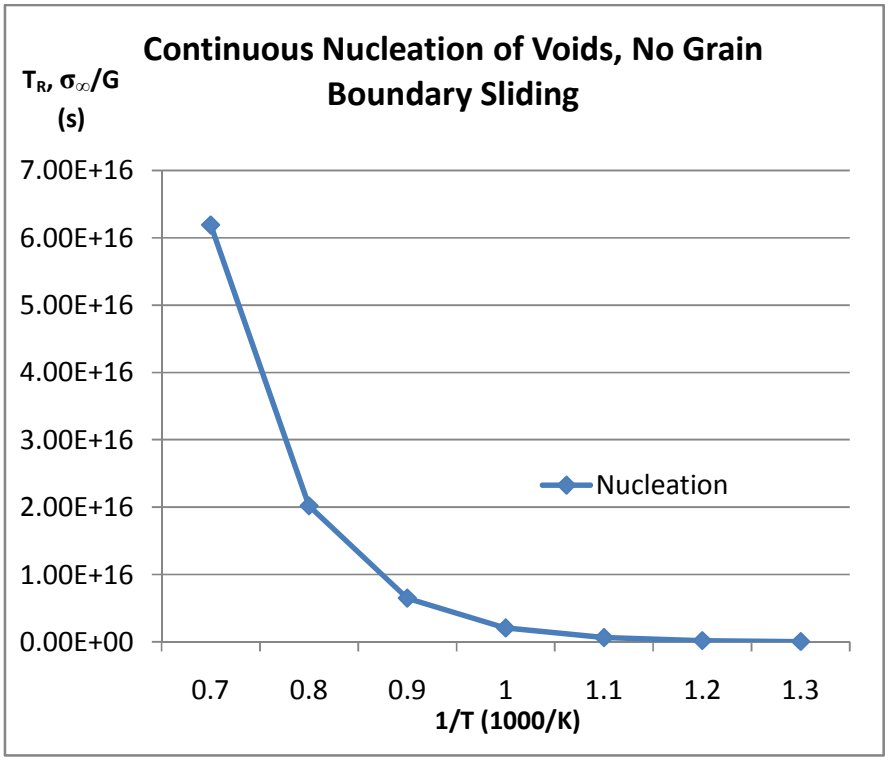

Figure 4.5: Continuous Nucleation, No Grain Boundary Sliding

The result for the time to rupture for continuous void nucleation and growth is not as per expected in Figure 4.4.The "U" trend was not replicated correctly. This

is due to the fact that several equations and constants were not provided and because of lack of information, radius of the voids, r at the start of nucleation and the increment of void density was not successfully obtained.

Due to this, the remaining area at the site could not be estimated. This lead to the nucleation rate not functioning properly and the result obtained would surely different than what it should be.

CHAPTER 5

5. CONCLUSION& RECOMMENDATIONS

5.1 Relevancy to the Objectives

The modeling of intergranular fracture at elevated temperature was carried out by replicating the models from the journal article, "Intergranular fracture at elevated temperature" by Rishi Raj and M. F. Ashby. It is anticipated that this model will help the estimation of the time to rupture for various metals; especially the ones operating at elevated temperatures as this type of metals are more expensive. Thus, the cost of maintenance and replacements of the components can be controlled.

Based on the results obtained, Raj & Ashby's results were modeled successfully for growth part. The model is able to replicate the original result and by using several another data for austenitic stainless steel, which is a material used in steam methane reformers. The results indicate that the critical region of the tube is the inside wall where the calculated time-to-rupture was lowest despite the fact that the temperature at this location was not the highest.

Although the nucleation model was not successful, the base line of the models which is the double integration function was already developed. The double integration function was successfully done and could function correctly if the radius and the void density increment could be determined and proper constants were available.

5.1 Recommendations

In order to improve the project progress and result, there are several recommendations that need to be considered which are:

1) Since programming is not a strong suit of a mechanical degree program, extra study and practice is needed regarding writing the code of numerical model of nucleation, growth and coalescence of voids.
2) Extra work is necessary to track and identify the equations used in continuous nucleation, no grain boundary sliding through the references listed by the author of Intergranular Fracture at Elevated Temperature, Rishi Raj and M.F Ashby [1].
3) Improvement of the models should be attempted occasionally to ensure the results of modeling will be accurate and satisfactory.
4) Repetition of modeling with several other materials data to ensure accuracy of model developed.

REFERENCES

[1] Rishi Raj and M.F Ashby (1975).Intergranular fracture at elevated temperature.Acta Metallurgical Vol. 23, 653-666.

[2] William D Calister, Jr. (2007). Materials Science and Engineering: An Introduction, 7th edition. John Wiley and Sons, Inc.

[3]Dr. SabbahAtaya, "Creep Testing Machines", 2008. Retrieved June 20, 2012, from http://www.slideshare.net/ea2m/creep-testing-machines-presentation

[4]"Structural Relaxation Due to Creep Impacts Performance".Retrieved Dec 14, 2012, from http://www.ansys-blog.com/2012/06/13/structural-relaxation-creep/

[5]NikAfifiNik Rahim (2010). Stress Analysis of Steam Methane Reformer Tubes. UTPedia.

[6] Carl Branan (2005). Rules of Thumbs for Chemical Engineers: A Manual of Quick, Accurate Solutions to Everyday Process Engineering Problems. Gulf Professional Publishing

[7] V.M Radhakrishnan (1986). Rupture life of materials obeying exponential and power law creep, Transactions ISIJ, Vol. 26.

[8] Y. Huang and A. Chandra (1998). Void-nucleation vs void-growth controlled plastic flow localization in materials with nonuniform particle distribution. Int. J. Solids Structures Vol.35, No.19, pp. 2475-2486.

[9]M. Kawai (1998). History-dependent coupled growth of creep damage under variable stress conditions. Metals and Materials, Vol. 4, No. 4, pp. 782-788.

[10] “Inspection of Steam Reformers and Catalyst Tubes with Infrared Thermography”. Retrieved Dec 13, 2012, from http://www.irinfo.org/articles/2_1_2008_james.html.

APPENDIX

Table A.1: Data Sheet for Copper

No	Symbol	Raj & Ashby (Cu)	Remarks
1	amu	63.55	atomic mass, $gmole^{-1}$
2	density	8.93E+06	atomic density, gm^{-3}
3	η	6.02E+23	Avogadro's number
4	Ω	1.10E-29	atomic volume, m^3
5	k	1.38E-23	Boltzmann's constant, JK^{-1}
6	R	8.314	gas constant, $Jmol^{-1}K^{-1}$
7	δ	4.00E-10	assumed GB thickness, m
8	T	973	absolute temperature, K
9	data type	B	A (estimation) or B (handbook)
12	D_B	1.70E-16	GB diffusivity cons, m^3s^{-1}
13	Q_B	1.04E+05	GB activation energy, $Jmol^{-1}$
14	δD_B	4.00E-15	GB diffusivity, $m^3\ s^{-1}$
16	$\sigma\infty$	4.20E+06	applied stress, N m^{-2}
17	γ	0.78	surface free energy, J m^{-2}
18	void type	A	A (β is active)
19	β (deg)	60	void geometry param
20	θ (deg)	60	
21	F_v	0.654498469	
22	F_b	2.35619449	
24	ρ	1.00E+10	void density, m^{-2}
25	l	5.00E-06	void-to-void distance, m
26	r_c	0.00000001	critical void radius, m
27	Δdt	3600	time step increment
28	A_{min}	0.0002	
29	n	1000	
30	h	2.00E-04	
31	G	4.2E9	

Table A.2: Data Sheet for Austenitic Steel

No	Symbol	N1-I	N1-min	N1-O	Remarks
1	amu	55.85	55.85	55.85	atomic mass, g $mole^{-1}$
2	density	7870000	7870000	7870000	atomic density, g m^{-3}
3	η	6.022E+23	6.022E+23	6.02E+23	Avogadro's number
4	Ω	1.1784E-29	1.1784E-29	1.18E-29	atomic volume, m^3
5	k	1.381E-23	1.381E-23	1.38E-23	Boltzmann's constant, J K^{-1}
6	R	8.314	8.314	8.314	gas constant, J mol^{-1} K^{-1}
7	T	1048.35493	1086.67993	1121.355	absolute temperature, K
8	(δDb)0	2E-14	2E-14	2E-14	GB diffusivity constant, m3 s^{-1}
9	Qb	169500	169500	169500	GB activation energy, J mol^{-1}
10	σ∞	113698371	2087663.92	83074397	remote applied stress, N m^{-2}
11	p	0	0	0	pressure inside of voids
12	void type	A	A	A	void geometry parameter - choices: 2 (0<a2<90 is active); 3 (30<a3<90 is active); 4 (30<a4<90 is active); A (0<β<90 is active); B (0<θ<90 is active)
13	a2 (deg)	45	45	45	
14	a3 (deg)	60	60	60	
15	a4 (deg)	60	60	60	
16	β (deg)	45	45	45	
17	θ (deg)	45	45	45	
18	Fb	1.57079633	1.57079633	1.570796	
22	l	0.00004	0.00008	0.00008	void-to-void distance, m
23	rB	2.5E-09	2.5E-09	2.5E-09	projected radius on GB, m
24	rc	2.5E-09	2.5E-09	2.5E-09	critical void radius, m
25	Amin	3.9063E-09	9.7656E-10	9.77E-10	Amin=(rB/l)2
26	Amax	0.5	0.5	0.5	arbitrarily set at 0.5
27	n	1000	1000	1000	integral steps
28	G	3.9E9	3.9E9	3.9E9	